Shell-Based Finite Element Modelling of RC Flat Plates Subjected to Non-uniform Connection Region Stresses

R. Abolhelm and T. D. Hrynyk

1 Introduction

Reinforced concrete (RC) flat plate construction is typical in modern building applications throughout much of the world. While RC flat plates are generally characterized by efficient load-carrying capabilities and cost-effective construction, the presence of highly concentrated and complex three-dimensional loading conditions at the slab-column connection regions of these systems can lead to brittle punching-governed failures that can propagate structural collapse [1]. Continued research in the area of RC slab punching is motivated by several factors, many of which relate to the fact that existing punching design provisions have been developed on the basis of experimental findings obtained from the testing of idealized RC slab-column connection specimens that only loosely represent the construction details and support/loading conditions that are experienced by real-world RC flat plates. More specifically, the data that have been used to inform today's design requirements, have almost entirely entailed isolated (i.e., single column) RC slab-column connections constructed with equal reinforcement ratios in orthogonal planar directions of the slab, and loading/support conditions that are intended to simulate the presence of square or circular intersecting columns. While these reinforcement and support conditions can, and do, exist in real-world flat plates, it is also quite common for RC flat plates to possess different ratios of steel in the orthogonal directions and/or be supported on rectangular columns with varied aspect ratios.

Recent studies aimed at investigating the punching shear resistance of slabs possessing rectangular supports, direction-varied reinforcement conditions, and/or non-uniform loading conditions have shown that these types of scenarios can cause highly non-uniform shear demand distributions to develop along the perimeters of

R. Abolhelm (✉) · T. D. Hrynyk
Department of Civil and Environmental Engineering, University of Waterloo, Waterloo, Canada
e-mail: reza.abolhelm@uwaterloo.ca

supporting columns and, as a result of this, existing punching design provisions do not provide the same level of conservatism as is obtained for the more typical idealizations noted above [2]. Further, recent numerical studies have also highlighted challenges in applying nonlinear finite element analyses (NLFEA) procedures to assess the performance of RC slab-column connections that experience highly non-uniform shear stresses along the perimeter of the column, as a result of column geometry or slab reinforcement condition. More specifically, it has been shown that NLFEA modelling techniques that have been employed successfully with more typical idealized slab-column connections involving square columns and symmetric reinforcement and loading conditions do not capture the structural performance of alternative connection details with the same level of precision and, in some cases, require the use of supplemental failure criteria to obtain meaningful results [3].

In this paper, the suitability of using a simple and low-cost thick-shell finite element modelling procedure to capture the punching shear resisting performance of RC flat plates subject to highly non-uniform shear stresses along the column perimeter as a result of geometric, reinforcement, or loading conditions is examined. In total, connection performance data pertaining to sixteen isolated slab-column connection specimens that were obtained from three test series presented in the literature were used to assess numerical response estimates developed using the software program VecTor4. Note that in all cases, the modelling approach, the behavioural models, and analysis parameters employed in the analyses were predefined and based on those used in prior VecTor4 modelling applications. The overarching objective of this paper is to determine if the thick-shell modelling procedure comprising VecTor4 can be used to cost-effectively estimate the performance of RC flat plates without the need for case specific calibration.

2 Background

2.1 RC Slab Analysis Procedure

Software program VecTor4, is a NLFEA procedure that is principally-dedicated to the assessment of RC planar structures, such as slabs and shells. It was originally developed on the basis of the shell structure analysis procedure developed by Figueiras and Owen [4]; however, has undergone progressive development and expansion over the past several decades in an effort to improve its assessment capabilities and to broaden its range of application [5–7]. Employing a layered thick-shell element, through-thickness structure composition (e.g., concrete and reinforcement layout) and response characteristics (e.g., stress, strain, stiffness) are considered explicitly and are calculated on the basis of the assumptions that (i) plane sections remain plane, but not necessarily normal to the element's in-plane mid-surface, (ii) out-of-plane (i.e., through-thickness) transverse normal stresses are negligible, and (iii) the 'effective' out-of-plane shear strain variation through the thickness of the shell

is parabolic. These assumptions are enforced by Reissner–Mindlin displacement field compatibility modelling [6, 8, 9], with additional modifications as presented in Hrynyk and Vecchio [10]. In-plane reinforcement, in any planar orientation, is incorporated using additional shell element layers that are also subject to assumptions i-iii and are positioned discretely within the thickness of the element. Out-of-plane reinforcement, if present, is incorporated in an entirely smeared sense and is uniformly distributed throughout the core concrete layers (i.e., layers not representing concrete cover regions) of the shell elements. As compared to commonly employed 3D solid continuum finite element modelling and as a result of the assumed through-thickness response conditions summarized above in assumptions i-iii, the number of required degrees of freedom and, as such, the computational requirements associated with VecTor4 models are significantly reduced; thus, enabling reduced computation costs. For the analyses presented in this paper, the commercially available pre- and post-processor program GiD was used to create all VecTor4 models.

2.2 Cracked RC Constitutive Modelling

VecTor4 program uses the Disturbed Stress Field Model (DSFM) [11] for the basis of cracked RC material modelling. The DSFM is an extension of the Modified Compression Field Theory (MCFT) [12] and comp rises a smeared, hybrid rotating-/fixed-crack modelling approach that inherently incorporates changes in material stiffness stemming from concrete cracking or crushing, steel yielding , post-cracking tension-stiffening, and the influence of concrete cracking on concrete compression response and shear-slip behaviour of cracked RC at crack surfaces. A detailed presentation of the DSFM, as modified to accommodate three-dimensional material modelling and as implemented in the thick-shell analysis program VecTor4, is available elsewhere [7].

In addition to the constitutive formulations of the DSFM, a number of supplemental material models are used to capture aspects of response that are not inherent to DSFM/MCFT material modelling, such as concrete confinement, dilatation, phases of unloading and reloading of the concrete and steel reinforcement, and plain concrete tension softening. In many cases these supplemental material models have only secondary impacts on the estimated response; however, in the case of RC flat plates constructed without shear reinforcement, influences stemming from local concrete expansion and confinement, as well as plain concrete tension softening, can be significant. A summary of the supplemental material models considered for all of the analyses presented in this paper are shown in Table 1. Note that these models are the same as those considered in Hrynyk and Vecchio [10] and, with only one exception, represent the 'default' material models that have typically been employed in VecTor4 validation studies. The concrete compression base curve is often selected on the basis of concrete compression strength. In this paper, Hognestad's parabola was used to model the compression base curve response for all specimens considered, regardless of concrete compressive strength.

Table 1 Key supplemental
material models

Material	Model	Description
Concrete	Compression base curve	Hognestad (parabola)
	Compression post peak	Modified Park-Kent
	Compression softening	Vecchio 1992-A
	Tension stiffening	Modified Bentz 2003
	Tension softening	Linear
	Confinement strength	Kupfer / Richart
	Concrete dilatation	Variable - orthotropic
	Cracking criterion	Mohr–Coulomb (Stress)
	Crack slip calculation	Basic (DSFM/MCFT)
	Crack width check	Crack limit (Agg/2.5)
	Hysteretic response	Nonlinear w/ offsets
Steel	Hysteretic response	Seckin (w/ Bauschinger)
	Dowel action	Tassios (crack slip)

Note: details pertaining to model formulations and
implementation are available elsewhere [13]

2.3 Treatment of Disturbed Regions

The equilibrium and compatibility conditions governing the formulation of the thick-shell modelling procedure employed in VecTor4 requires that plane sections remain plane (assumption i noted above in Sect. 2.1) and that out-of-plane normal stresses sum to zero (assumption ii from 2.1). However, slab-column connection regions comprising RC flat plates are highly disturbed regions where transverse confinement and direct strut action are known to occur, and can contribute to suppressing the development of tension-governed shear failures within these regions. To account for these beneficial out-of-plane shearing effects, VecTor4 employs a form of local out-of-plane shear strain suppression within the disturbed regions of slabs using the methodology presented in Goh and Hrynyk [7]. Note that the treatment of connection disturbed regions is critical to the shell-based modelling of RC slabs that are shear sensitive punching and, as such, is automated within VecTor4 using a procedure that requires no additional costs from a user modelling perspective or run-time.

3 Shell-Based Modelling of RC Slabs with Non-uniform Punching Shear Stresss Conditions

Prior VecTor4 applications involving RC slab punching have generally demonstrated that the modified thick-shell finite element analysis procedure employed is capable of estimating the punching capacity of RC slab-column connections with levels of precision and accuracy matching those obtained using more costly 3D NLFEA modelling procedures [14]. However, in these prior studies, the test slabs used for validation consisted of slab-column connection specimens with square intersecting column geometries and equal reinforcement ratios in the planar direction. As a result, the punching shear stresses developed in these connections were well-distributed along all faces of the column perimeter, with limited influence of shear stress localization. In this paper, thick-shell NLFEA validation studies comprising three different testing programs were carried-out to investigate the suitability of using VecTor4 to estimate the punching performance of slabs supported on rectangular columns, slabs subjected to non-uniform loading conditions, and slabs constructed with unequal planar reinforcement ratios: (i) a series of five slabs supported on rectangular columns with different aspect ratios and subjected to well-distributed two-way loading conditions [15], (ii) seven square column-supported slabs that were constructed with different orthogonal reinforcement ratios and were subjected to different loading conditions producing variable shear stress distributions around the supporting column connections [16], and (iii) four slab-column connections with rectangular supports subjected to non-uniform shear loading conditions [17]. Note that in all of the tests considered, the slab-column connection specimens were constructed without through-thickness shear reinforcement.

3.1 Oliveira et al. Rectangular Column Supported Slabs

Oliveira et al. [18] reported the findings from the testing of three series of isolated slap punching specimens. In total, fifteen rectangular high-strength RC slab specimens, measuring 2280×1680 mm in plan, with thicknesses of 130 mm, were subdivided into three series of tests: test series A consisted of slabs subjected to predominantly one-way loading in a manner that produced slab bending about the longer spanning direction, test series B involved slabs subjected to bending about the shorter spanning direction, and test series C involved slabs subjected to well-distributed two-way loading conditions. In all cases, the slabs were supported on rectangular columns with column aspect ratios (i.e., the ratio of column long face to short face) ranging from one to five. The slabs were reinforced with regularly spaced 12.5-mm diameter bars resulting in a reinforcement ratio of approximately 1.1% in the two planar directions. The concrete compressive strength ranged from 54 to 63 MPa, and the slabs were constructed with a concrete mixture employing a maximum nominal aggregate size of 16 mm. In all cases, the slabs exhibited brittle punching shear

failures. Key results from the study suggested that existing code provisions had the tendency to overestimate punching resistance. For brevity, only the results from the two-way loaded series C tests are presented below. Note that a thick steel bearing plate was used to simulate the presence of an intersecting column and the slabs were loaded along their perimeters using a series of 8 equal magnitude concentrated forces that were applied to stiff loading beams acting on each edge of the slab. An overview of the properties of the C series slab are reported in Table 2.

3.1.1 Modelling Approach

Taking advantage of symmetric geometry and loading conditions, a one-quarter finite element mesh was created for each C-series slab specimen. Constrained lateral in-plane displacements and corresponding rotations were assigned to enforce symmetry conditions. Shell finite element sizing of 25 mm (~ 23% of d_{eff}) to 50 mm (~ 47% d_{eff}) in plan were used in the slab modelling, with the finer elements being employed in the slab regions surrounding the columns and the more coarse elements being provided toward the free edges of isolated slabs. An unstructured mesh, developed using the element size to point technique within the software program *GiD*, was applied to vary the mesh density within critical and non-critical regions of the test specimens. The total number of shell elements comprising the models was on the order of about 435, requiring 8,900 total degrees of freedom. Each layered shell element was subdivided into 20 equal-thickness concrete layers, and an additional four layers were used to represent in-plane reinforcement at different depths (two tension side layers and two compression side layers). Note that, in comparison to more conventional 3D solid continuum finite element modelling, these models require far fewer degrees of freedom and, as a result, the total run-time for each nonlinear analysis was less than an hour, with use of a typical personal laptop computer (ASUSTek (UX410U NotebookPC): Intel Core i7-8550U CPU @ 1.80 GHz, RAM: 16 GB). The test specimen geometry and a typical shell element mesh employed for the Oliveira et al. slabs are shown in Fig. 1.

   In addition to applying the slab self-weight by way of body loads, the one-quarter slab models were loaded at two points using a master–slave displacement-controlled loading method where one concentrated loading point is defined by prescribed nodal displacements (i.e., the master node) and the second concentrated load (the slave node) mirrors the force required to impose the displacement at the master node. In all case, the perimeter loading beams were neglected, as prior studies indicated that the consideration of these beams had negligible impact on computed response [3].

3.1.2 Results

Numerical shear (V) versus vertical displacement responses obtained for each of the slabs are plotted alongside the reported experimental results in Fig. 2. From the results presented in this figure, it can be seen that VecTor4 captured the brittle
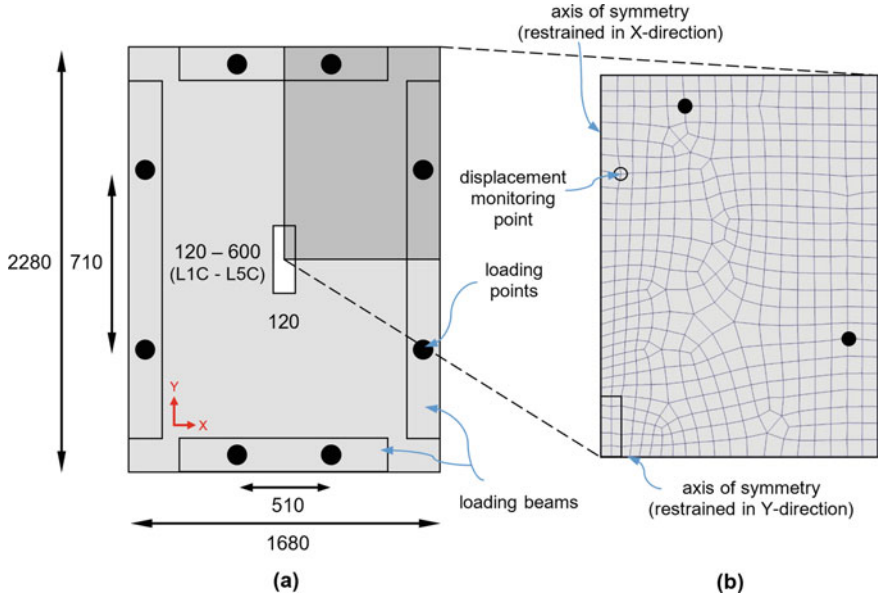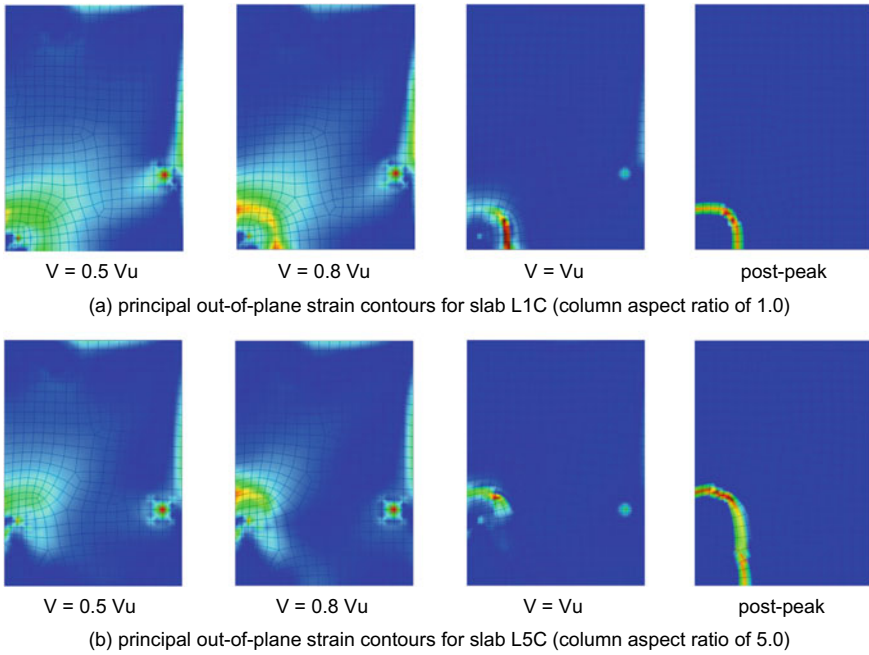
Fig. 1 Illustration of Oliveira et al. test specimens **a** geometry; **b** typical mesh (L3C) [all dimensions are shown in unit of mm]
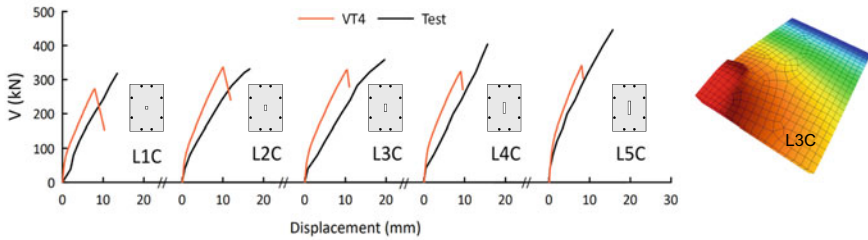
Fig. 2 Shear-displacement responses for Oliveira et al. slabs (L1C–L5C)

punching shear failure modes that were reported to govern slabs L1C-L5C. Note that to clearly demonstrate the brittle punching failure modes computed for the slabs, partial post-peak stages of response have been included. The reported experimental data did not include the post-peak phases of response. From the comparison of the average through-thickness shear strain distributions obtained in the slab-column regions for L1C and L5C (illustrated in Fig. 3), columns with increased aspect ratios were estimated to develop increased shear demands along the short sides and the corners of the supports, and the punching shear failures were estimated to initiate in the slab region adjacent to the short side of the rectangular columns and then propagate around the full parameter of the supporting. Finally, it can be seen that while increasing the column size (and aspect ratio) led to significant shear strength gains

| V = 0.5 Vu | V = 0.8 Vu | V = Vu | post-peak |

(a) principal out-of-plane strain contours for slab L1C (column aspect ratio of 1.0)

| V = 0.5 Vu | V = 0.8 Vu | V = Vu | post-peak |

(b) principal out-of-plane strain contours for slab L5C (column aspect ratio of 5.0)

Fig. 3 Influence of column aspect ratio on shear distribution surrounding column

in the experimental program, the ultimate shear resistance estimated using VecTor4 showed only marginal increases in slab capacity with increasing column size/aspect ratio. For the five Oliveira et al. slabs considered, the mean computed-to-reported punching capacity ratio was found to be 0.87, with a coefficient of variation (CoV) of 10.5%. Note that Table 2 presents a summary of the capacity results obtained, as well as several key parameters, for each slab.

3.2 Sagaseta et al. (2011, 2014) EPFL Slabs

Two series of isolated slab-column connections with uniform geometry were tested at École Polytechnique Féderale de Lausanne (EPFL) to examine the influence of different loading patterns, column aspect ratios, and slab reinforcement ratios on connection shear resisting performance. In the PT series of tests, seven square slabs, measuring 3000 × 3000 mm in plan and 250-mm thick, were supported on 260-mm square column supports and were constructed without any form of out-of-plane reinforcement. This series of slabs was tested to investigate the effect of non-uniform punching shear stress development in specimens constructed with squares columns and different reinforcement ratios in the planar directions (PT21-PT33) or specimens with square supporting columns and subjected to non-symmetrical loading (PT34).

The longitudinal reinforcement ratios comprising the slabs ranged from 0.32% to 1.64%. In the AM series of tests, four slab-column connections with the same dimensions as the PT series slabs were constructed with 0.75% longitudinal reinforcement in both planar directions, and were supported on rectangular columns measuring 260 × 780 mm. The AM series slabs were tested under different out-of-plane loading patterns. Specimens AM01, AM02, and AM03 were loaded at four points along two-edges, and AM04 was loaded at eight points that were equally spaced along the perimeter of the specimen. Additional details pertaining to the AM and PT EPFL tests are presented in Table 2.

3.2.1 Modelling Approach

The same general meshing technique as that reported for the Oliveira et al. slabs was used to model the Sagaseta et al. EPFL slabs. One-quarter slab-column connection models were created using an unstructured mesh. A shell element size of 50 mm (~ 24% of d_{eff}) was employed in the slab regions surrounding the supporting columns and maximum size of about 100 mm (~ 48% of d_{eff}) was used along the less critical edge regions of the slabs. As the geometry of slabs and the supporting column was constant in each of the PT and AM testing programs, only one finite element mesh was required for each series. A total of 275 shell elements were employed in the PT series slab modelling and 251 shells were required for the AM slabs. For both the PT and AM slab models each layered shell element was subdivided into 20 equal-thickness concrete layers, and an additional four layers were used for in-plane reinforcement.
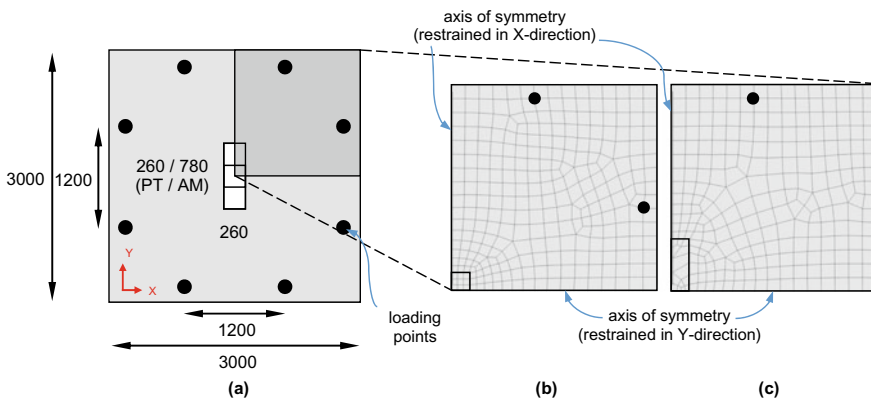
Fig. 4 Illustration of Sagaseta et al. [16, 17] test specimens **a** geometry; **b** finite element mesh for PT21; **c** finite element mesh for AM02 [all dimensions are reported in units of mm]

3.2.2   Results

Figures 5 and 6 present the numerical shear (V) versus vertical slab rotation (ψ) responses obtained alongside the reported experimental results for the PT and AM slabs, respectively. Recall that for these two EPFL series of tests, a single finite element mesh was used within each series. Note that for the numerical calculation of slab rotations, the North–South and East–West rotations were calculated along the axes of symmetry in the X- and the Y-directions, at the location of the free edges of the quarter slab models.

From the results presented in Fig. 5, it can be seen that load-rotation responses of the PT slabs were generally captured well. The computed initial/pre-yield stiffnesses of slabs were in good agreement with that reported and, in the majority of cases (i.e., PT21, PT22, PT33, and PT34) the punching shear resistance was estimated with high accuracy. The effect of reinforcement variation on the results of the analysis seemed to be negligible. In the case of slabs PT31 and PT32, it can be seen that VecTor4 provided significant strength underestimations. It is unclear what the cause of the strength underestimation is for these two slabs; however, it should be noted that the results obtained by others using calibrated high resolution 3D solid NLFEA also reported significant underestimations for the capacities of these slabs. The mean
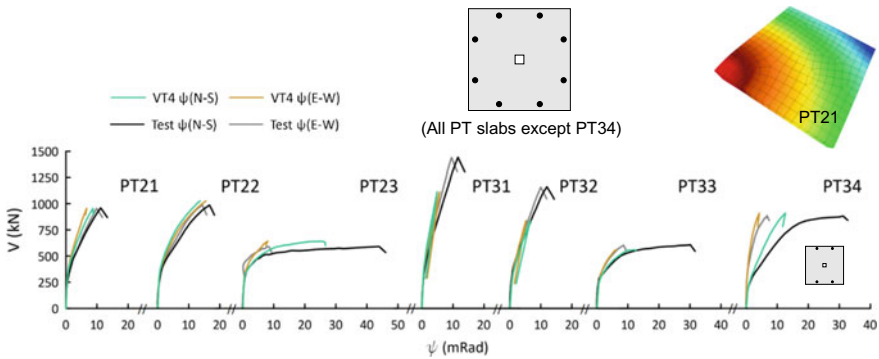

Fig. 5 Shear-displacement responses for Sagaseta et al. [16] slabs (PT21 – PT23; PT31 – PT34)
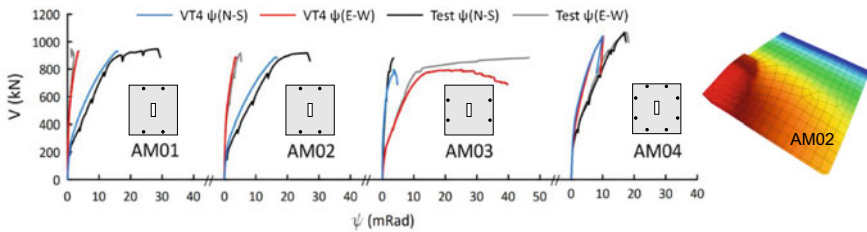

Fig. 6 Shear-displacement responses for Sagaseta et al. [17] slabs (AM01 – AM04)

Table 2 Summary of test specimen characteristics and capacity results

Specimen	Load*	d (mm)	ρ_x (%)	ρ_y (%)	f'_c (MPa)	$Column$: (mm) $C_{max} \times C_{min}$	V_{test} (kN)	V_{VT4} (kN)	V_{VT4}/V_{Test}
Oliveira et al. [15]									
L1C	TW	107	1.09	1.09	59.0	120 × 120	318	273	0.86
L2C	TW	107	1.09	1.09	57.0	240 × 120	331	336	1.02
L3C	TW	106	1.10	1.10	54.0	360 × 120	358	329	0.92
L4C	TW	107	1.09	1.09	56.0	480 × 120	404	323	0.80
L5C	TW	109	1.07	1.07	63.0	600 × 120	446	341	0.76
Sagaseta et al. [16]									
PT21	TW	192	1.64	0.84	67.5	260 × 260	959	955	1.00
PT22	TW	196	0.82	0.82	67.0	260 × 260	989	1026	1.04
PT23	TW	189	0.85	0.36	66.0	260 × 260	591	641	1.08
PT31	TW	212	1.48	1.48	66.3	260 × 260	1433	1111	0.78
PT32	TW	215	1.46	0.75	40.0	260 × 260	1157	840	0.73
PT33	TW	212	0.76	0.32	40.2	260 × 260	602	561	0.93
PT34	OW	216	0.74	0.74	47.0	260 × 260	879	910	1.04
Sagaseta et al. [17]									
AM01	OW	214	0.75	0.75	44.0	780 × 260	950	931	0.98
AM02	OW	208	0.75	0.75	39.7	780 × 260	919	888	0.97
AM03	OW	203	0.75	0.75	42.2	780 × 260	883	797	0.90
AM04	TW	202	0.75	0.75	44.6	780 × 260	1067	1038	0.97
							Mean =		0.92
							CoV* (%) =		11.5

* OW = one-way loading; TW = two-way loading; CoV = coefficient of variation
Additional notes:
- For all slabs, the maximum nominal course aggregate size, d_{agg}, was reported to be 16 mm
- Yield stress for x-direction bars (f_{yx}) was 597, 552, 552, 540, 540, 558, 558 MPa for slabs PT21 to PT34, respectively
- Yield stress for y-direction bars (f_{yy}) was 552, 552, 568, 540, 558, 533, 558 MPa for slabs PT21 to PT34, respectively

computed-to-reported shear capacity ratio for the seven PT slabs was 0.94, with a CoV of 13.5%.

On the basis of the results presented in Fig. 6, it can be seen that VecTor4 was able to accurately estimate the response of the rectangular column supported AM series of slabs. In all cases, estimates of the initial slab stiffness were captured well and the estimated governing modes of failure (e.g., brittle punching vs. flexural yielding followed by punching) were in agreement with those reported experimentally. It can also be seen that the capacities of slabs were captured with high accuracy. Further, while longitudinal steel yielding was estimated to occur prior to the onset of punching in slabs AM02 and AM03, the ductile responses exhibited by these slabs was not

captured numerically. In all, the mean computed-to-experimentally reported strength ratio of the AM series slabs was 0.96 with a CoV of 3.4%. A summary of the results obtained for all of the PT and AM slabs is reported in Table 2.

4   Conclusion

The thick-shell NLFEA program VecTor4 was used to analyze sixteen slab-column connection specimens under concentric shear loading conditions that, as a result of column geometry, slab reinforcement conditions, and/or loading conditions, developed highly non-uniform shear demands along the perimeters of the supporting columns. The overarching goal of this study was to determine if VecTor4 can be used to cost-effectively estimate the performance of RC flat plates without the need for case specific model calibration. On the basis of the results presented, the following main conclusions can be drawn:

- NLFEA employing thick-shell elements can be used to cost-effectively estimate the punching shear resisting performance RC slabs and slab systems. The level of precision and accuracy obtained for the atypical slab-column connection tests considered in this paper is comparable to numerical results obtained by VecTor4 for more common idealized slab-column connections. In all, a mean numerically estimated-to-experimentally reported capacity ratio of 0.92 was obtained with a CoV of 11.5%.
- Despite the fact that no model calibration was performed, the DSFM-based concrete material modelling was capable of estimating the governing modes of response with high accuracy in all cases. In agreement with reported experimental results, punching failures were estimated to occur in all of the slabs and yielding of the longitudinal reinforcement was captured in all of the slabs that were reported to exhibit ductile responses.
- Of the different test series considered, the Oliveira et al. two-way slab specimens proved to be the most challenging to estimate numerically using VecTor4. In this series, VecTor4 did not capture the level o f strength increase attributed to increased column size when the aspect ratio of the column was also increasing.

References

1. Mitchell D, Cook WD (1984) Preventing progressive collapse of slab structures. J Struct Eng ASCE 110(7):1513–1532
2. Milligan GJ, Polak MA, Zurell C (2020) Finite element analysis of punching shear behaviour of concrete slabs supported on rectangular columns. J Struct Eng, ASCE, 224:111189
3. Setiawan A, Vollum RL, Macroini L, Izzuddin A (2020) Punching of RC slabs without transverse reinforcement supported on elongated columns. Structures 27:2048–2068

4. Figueiras JA, Owen DRJ (1984) Analysis of elasto-plastic and geometrically nonlinear anisotropic plates and shells. In: Hinton E, Owen DRJ (eds) Finite element software for plates and shells. Pineridge, Swansea, UK
5. Polak MA, Vecchio FJ (1993) Nonlinear analysis of reinforced concrete shells. J Struct Eng ASCE 5(655):655–664
6. Hrynyk TD, Vecchio FJ (2016) Modeling of steel-concrete composite elements under in-plane and out-of-plane loads. J Struct Eng ASCE 142(10):04016080
7. Goh CYM, Hrynyk TD (2020) Nonlinear finite element analysis of reinforced concrete flat plate punching using a thick-shell modelling approach. Eng Structures, Elsevier, 224
8. Reissner E (1945) The effect of transverse shear deformations of the bending of elastic plates. J Appl Mech, ASME 12:69–77
9. Mindlin RD (1951) Influence of rotary inertia and shear on flexural motions of isotropic, elastic plates. J Appl Mech, ASCE 18:31–38
10. Hrynyk TD, Vecchio FJ (2015) Capturing out-of-plane shear failure in the analysis of reinforced concrete shells. J Struct Eng ASCE 141(12):04015058
11. Vecchio FJ (2000) Disturbed stress field model for reinforced concrete: formulation. J Struct Eng, ASCE 126(9):1070–1077
12. Vecchio FJ, Collins MP (1986) The modified compression-field theory for reinforced concrete elements subjected to shear. ACI J 83(2):219–231
13. Wong PS, Vecchio FJ, Trommels H (2013) VecTor2 and formworks user's manual, 2nd edn. University of Toronto, Ontario, Canada
14. Goh CYM, Hrynyk TD (2018) Numerical investigation of the punching resistance of reinforced concrete flat plates. J Struct Eng ASCE 144(10):04018166
15. Oliveira DRC, Regan PE, Melo GSSA (2004) Punching resistance of RC slabs with rectangular columns. Mag Concr Res 56(3):123–138
16. Sagaseta J, Muttoni A, Fernandez Ruiz M, Tassinari L (2011) Non-axial-symmetrical punching shear around internal columns of RC slabs without transverse reinforcement. Mag Concr Res 63(6):441–457
17. Sagaseta J, Tassinari L, Fernandez Ruiz M, Muttoni A (2014) Punching of flat slabs supported on rectangular columns. J Struct Eng ASCE 77:17–33
18. Oliveira DRC (2003) Experimental analysis of reinforced high strength concrete flat slabs with elongated columns, PhD thesis, University of Brasilia, Brazil